Electrochemical immunosensor development with chitosan modified reduced graphene oxide-nanoceria nanocomposite for gentamicin detection

Jayendra Kumar Himanshu[1,2], G.B.V.S. Lakshmi[1,3], S. Z.H. Hashmi[1], Ahmed Kareem Hussein Alatafi[4] Akhilesh Kumar Singh[2*], Pratima R. Solanki[1*]

[1]Special Centre for Nanoscience, Jawaharlal Nehru University (JNU), New Delhi-110067, India.

[2]Department of Biotechnology, School of Life Sciences, Mahatma Gandhi Central University, Motihari, Bihar-845401, India.

[3]Department of Physics, Anurag University, Ghatkesar, Hyderabad, Telangana 501301, India

[4]Department of Biology, College of Science, University of Diyala, Diyala, Iraq

*Corresponding author email: partima@mail.jnu.ac.in; pratimarsolanki@gmail.com akhileshsingh@mgcub.ac.in; akhiliit@gmail.com

Supplementary information file

The CV data is showing CH-(rGO@CeO_2)/SPEs immunoelectrode was modified using a 3 mg/ml solution with a 5 µl deposition volume, ensuring uniform surface coating and efficient electron transfer properties. Different pH conditions (6.0, 6.5, 7.0, 7.4, and 8.0) were tested to determine the most favourable pH range for optimal sensor performance, as shown in Fig. S1. Based on the obtained results, the maximum current response was recorded at pH 7.

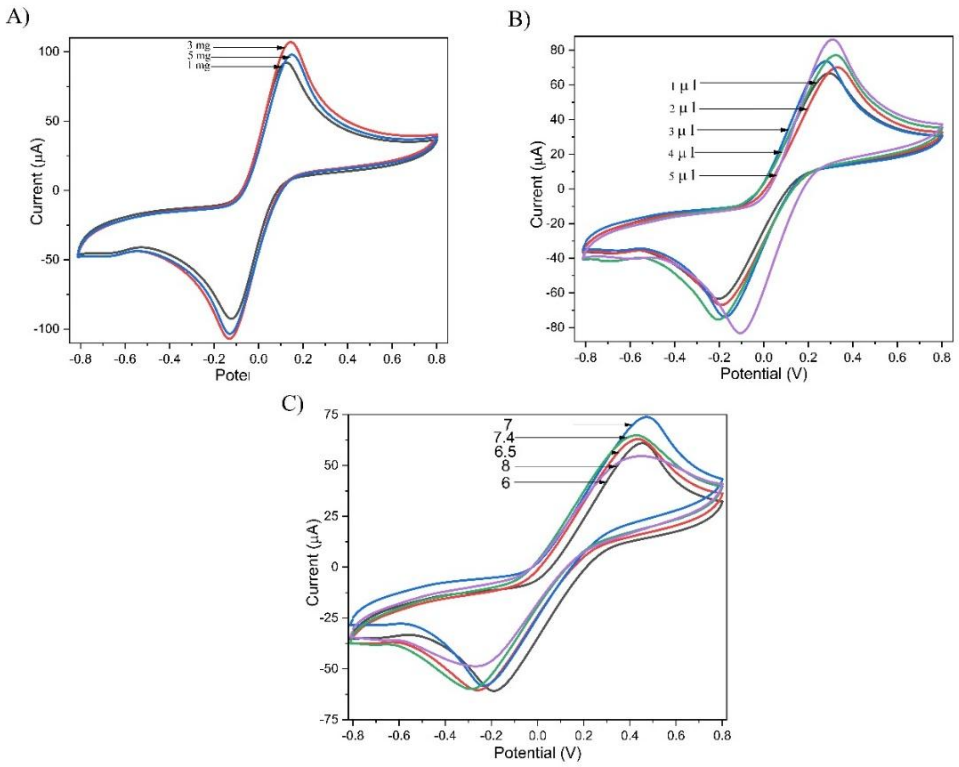

Fig. S1 Concentration (A) and (B) volume optimisation of CH-(rGO@CeO_2) on SPE and (C) pH conditions optimisation on BSA-anti-GEN/CH-(rGO@CeO_2)/SPE.

Electrochemical kinetics and redox features of Anti-GEN/CH-(rGO@CeO_2)/SPE and BSA-anti-GEN/CH-(rGO@CeO_2)/SPE enabling the assessment of electron transfer efficiency and surface interactions. The electrochemical study was carried out in PBS buffer solution with redox mediator at scan rates between 10 and 100 mV s^{-1} as shown in Fig. S2. These immunoelectrode reflects an efficient electron transport mechanism, promoting its suitability for rapid and sensitive electrochemical analysis.

Electrochemical characteristics of CH-(rGO@CeO_2), Anti-GEN/CH-(rGO@CeO_2), and BSA/Anti-GEN/CH-(rGO@CeO_2) immobilized on SPEs was examined using CV and DPV. These measurements provide insights into the electrode surface functionalization impact on charge transfer dynamics and biofunctionalization effects. As shown in Fig. S3, (a) the CV reveal a substantial change in peak current (b) as compared to Anti-GEN/CH-(rGO@CeO_2). Further decrease in the peak current (c) confirms BSA immobilization.

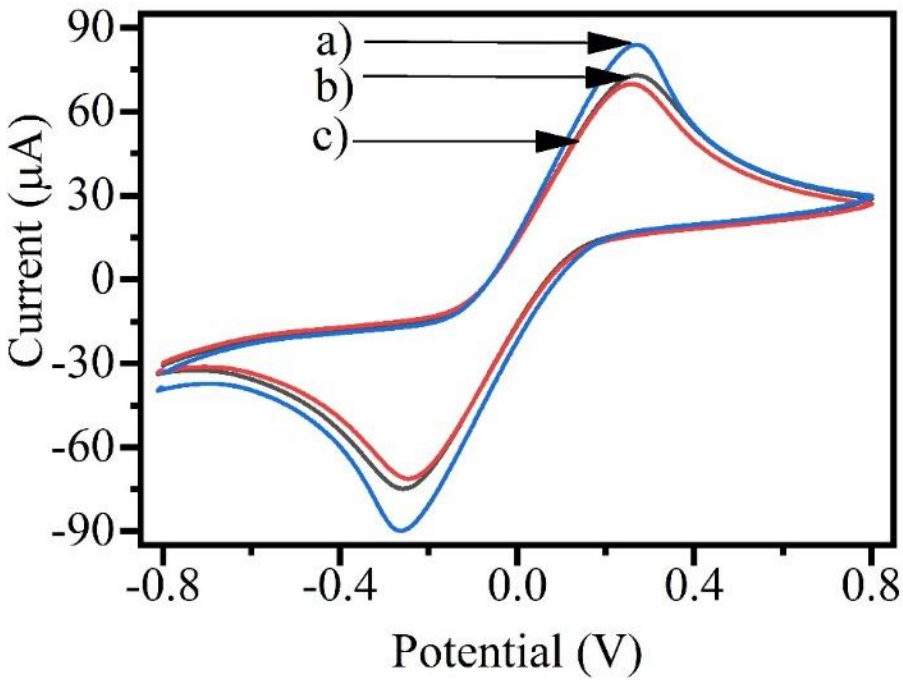

Fig. S2 The electrochemical properties of a) CH-(rGO@CeO_2)/SPE b) Anti-GEN/CH-(rGO@CeO_2)/SPE and c) BSA/Anti-GEN/CH-(rGO@CeO_2)/SPE were evaluated through CV at 50 mV/s.

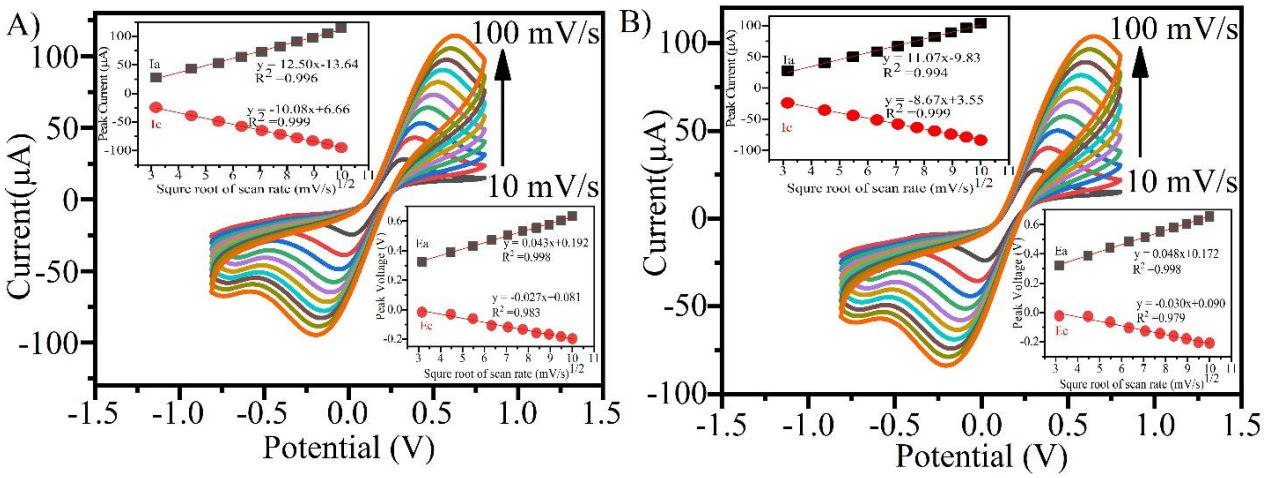

Fig. S3 Electro-kinetic study of A) Anti-GEN/CH-(rGO@CeO_2)/SPE (inset) square root of the scan rate and the peak current, as well as the peak voltage and B) BSA/Anti-GEN/CH-(rGO@CeO_2)/SPE (inset) square root of the scan rate and the peak current, as well as the peak voltage.

The spiked concentration, recovery percentage and relative standard deviation values obtained for spiked Milk and Tap water samples are given in Table S1. The values of recovery percentage and RSD are better in tap water samples than of Milk samples. This may be due to the presence of various high molecular weight biomolecules present in the milk samples hinder the current values.

Table S1 RSD%, spiked concentration and recovery percentage.

Concentration (nM)	Current of Standard (μA)	Current of Spiked (Milk) (μA)	Current of (Tap Spiked Water) (μA)	Detect Concentration (Milk) (nM)	Detect Concentration (Tap Water) (nM)	Recovery % (Milk)	Recovery % (Tap Water)	RSD % (Milk)	RDS % (Tap Water)
0.001	4.645	4.56504	4.592835	0.000983	0.000989	98.28	98.87	1.21	0.79
0.01	4.433	4.07376	4.24008	0.00919	0.009565	91.89	95.64	5.97	3.14
0.1	4.229	3.7398	4.05405	0.088432	0.095863	88.43	95.86	8.6	2.98
1	4.159	3.40032	3.3045	0.817581	0.929614	81.76	92.96	14.14	5.1
10	3.915	3.19884	3.866265	8.170728	9.014828	81.71	90.14	14.23	7.3
100	3.752	2.92836	3.529305	78.04797	86.11287	78.05	86.11	17.43	10.5
250	3.574	2.70204	3.230955	189.0067	212.2548	75.60	84.90	19.6	11.5
500	3.442	2.52816	3.034395	367.2516	416.8252	73.45	83.36	21.6	12.8
750	3.243	2.24388	2.869425	518.9362	661.1691	69.19	88.15	25.2	8.9
1000	3.075	2.20524	2.525445	717.1512	821.2829	71.71	82.12	23.21	13.87
10000	3.017	2.40805	2.406105	6440.305	7975.157	64.40	79.75	30	15.9